ISSN 2616-5791 Vol.5, Issue 5: 7-12, DOI: 10.25236/AJMHS.2024.050502

Nanomedicine enhanced photodynamic therapy for triple negative breast cancer

Zhong Jiayi[1,a,*]

[1]*Guangdong Experimental Middle School, Guangzhou, China*
[a]*Zhongjiayi070520@163.com*
[*]*Corresponding author*

Abstract: *In this study, we synthesized and prepared nanomedicines with microenvironment responsive and optical activity targeting the high ROS, hypoxic, and acidic characteristics of the tumor microenvironment. We speculate that using MOC-68 mediated photodynamic therapy to inhibit tumor growth, combined with hydrogen sulfide loaded donor DATS, and integrating hollow mesoporous MnO2 nanoparticles to improve PDT efficiency, while achieving MRI visualization monitoring of the treatment process. We conducted some preliminary experiments, and the research results preliminarily confirmed that the hypothesis of the topic is reasonable and has potential.*

Keywords: *Triple-negative breast cancer, Photodynamic therapy, nanodrugs, ROS*

1. Introduction

Breast cancer is the most common malignancy in women all over the world.[1] Triple-negative breast cancer (TNBC) is a vitally aggressive sub-type of breast cancer, which is responsible for approximately 15% of breast cancers. The negative expression of estrogen receptor, progesterone receptor, or human epidermal growth factor receptor-2 (HER-2) genes identify it.[2] This special type of tumor is well known of poor prognosis because of its only partial response to chemotherapy and lack of clinically practical targeted therapies. The median overall survival of TNBC is only approximately 1 year.[3]

Nowadays, TNBC patients can be treated with standard chemotherapy before or after surgery, but the majority of them sill face high risk of recrudescence and mortality due to the chemotherapeutic resistance.[4] The cause apparently lies in the therapy strategies. Current therapies for TNBC consist of the following, surgeries, neoadjuvant chemotherapy for early-stage disease, immunotherapy, such as CTLA4 and PD-(L)1 inhibitors and systemic therapy for metastatic disease (includes a taxeme or anthracycline combination).[5] They are fine, but all have their own drawbacks. Surgeries are most used, but due to some contraindications which must be treated in advance, the best cure time may be missed. Neoadjuvant anthracycline–cyclophosphamide (AC-scheme) chemotherapy appears to be establishing efficacy, although recently there have been reports on resistance developed for these drugs, leading to efficacy loss.[6] The current efforts of immunotherapy are directed to activate immune system response by using CTLA-4 inhibitors such as ipilimumab, but they activate T-cells in an aggressive way, generating different systemic adverse effects, represented by cytokine storm.[7]Thus, though various treatment methods are designed, an apparent and vital need to develop other new therapeutic strategies for TNBC still exists.Therefore, a newly developed strategy, photodynamic therapy, has its own advantages.

In recent years, numerous studies have shown that various cells and extracellular matrix components in the tumor microenvironment (TME) play important roles in tumor development, invasion, metastasis, and the treatment of cancer.[8] Therefore, targeting the tumor microenvironment has become a new approach in the diagnosis and treatment of breast cancer. Drug delivery, release, and intervention targeting the characteristics of the TME and its different functional targets have become effective strategies in tumor treatment. Reactive oxygen species (ROS), as important regulatory factors in various cellular processes, have become a major target for TME treatment.[9] Although tumor cells have higher levels of ROS compared to normal cells, they also have higher antioxidant activity to maintain redox balance. A series of studies have shown that when the level of ROS exceeds a certain threshold, it can induce apoptosis in tumor cells without affecting normal cells.[10-12]

ISSN 2616-5791 Vol.5, Issue 5: 7-12, DOI: 10.25236/AJMHS.2024.050502

Additionally, due to rapid tumor growth and disrupted vascular systems, solid tumors contain many hypoxic regions.[13,14] Tumor cells can adapt and survive in hypoxic environments due to the Warburg effect.[13] Hypoxia-inducible factor-1 (HIF-1α), a transcription factor, is considered a major regulator of cellular adaptation to hypoxia.[13,14] Under hypoxic and metabolic stimuli, HIF induces tumor and stromal cells to secrete vascular endothelial growth factor (VEGF), which drives angiogenesis, promotes tumor cell invasion and metastasis, hinders drug delivery, and further exacerbates hypoxia in the TME.[14] Therefore, improving the hypoxic environment, downregulating the expression of HIF-1α, and inhibiting VEGF-mediated tumor angiogenesis have become major targets in cancer treatment.In recent years, photodynamic therapy (PDT) has received widespread attention due to its unique cytotoxic mechanism.[15] PDT generates a large amount of reactive oxygen species, which directly induce cell death in tumor cells (including apoptosis, autophagy, and necrosis), damages the tumor vascular system, and activates the immune system, leading to a strong inflammatory response.[16] Due to the unique anti-tumor mechanism of PDT and the lack of a mechanism to directly eliminate singlet oxygen in the tumor microenvironment, PDT can be repeated without causing drug resistance or poor response.[17,18] However, most photosensitizers have low tumor tissue targeting ability and cannot address the deficiencies of tumor tissue, such as hypoxia. In the past, the targeting of photosensitizers could be improved by usingpolymer delivery platforms triggered by acidity or protease expression in the tumor environment.[19] The newly developed ruthenium (II) based metal-organic cage (MOC) has optical activity, microenvironment responsiveness, and fluorescence imaging capabilities, and it tends to accumulate in environments rich in hydrogen peroxide. Furthermore, it can load small molecule drugs with controllable drug loading capacity, good biocompatibility, and the ability to release in response to the microenvironment. Hollow mesoporous MnO2 is often used as a carrier for nanomedicines. It can react with hydrogen peroxide (H2O2) under weakly acidic conditions to generate Mn^{2+} and O2. The generated oxygen can enhance photodynamic therapy and alleviate TME hypoxia. In practical applications, PDT is often combined with other treatment modalities for cancer treatment. Hydrogen sulfide has a good anti-tumor effect and can enhance the effect of photodynamic therapy by inhibiting the activity of hydrogen peroxide enzymes.[19] However, the hydrogen sulfide donor, diallyl trisulfide (DATS) extracted from garlic, reacts, and depletes rapidly in the blood circulation, making its precise delivery to tumor tissues limited and restricting its clinical application.[20]

2. Experimental Section

DATS-MOC@MnO2@PEG (DMM) were synthesized and prepared by the research team of the supervising teacher's laboratory. *Cell Culture and Treatment:* MDA-MB-231 cells (Human breast cancer cell) were obtained from the Cell Bank of the Chinese Academy of Sciences (Shanghai, China) MDA-MB-231and MCF-7 cells were cultured in media (DMEM, Gibco, USA) supplemented with 10% fetal bovine serum (Sigma–Aldrich, USA), 1% penicillin and streptomycin antibiotics (Sigma– Aldrich) in a humidified atmosphere with 5% CO2 and 95% air at 37°C. The cells were incubated at 37 °C in an anaerobic incubator (96.5% N2, 2.5% CO2, and 1% O2) to mimic a hypoxic environment.

MDA-MB-231 cells were incubated in 6-well plates (5 × 105 cells/well) for 24 hours and then treated with DATS (100 μM) and DMM (100 μM) for 12 hours. Subsequently, the DATS and DMM treated cells were subjected to 450-nm laser irradiation at 1 W/cm^2 for 10 min/well as experimental group (5 laser irradiation points/well). The DATS and DMM treated cells without laser irradiation or untreated cells without laser irradiation were as control group. *qRT-PCR:* TRIzol reagent (EZ-press RNA Purification Kit, EZBiosciences, USA) was used to extract total RNA. Next, the concentration of total RNA was measured by ultramicro spectrophotometer (N60 Touch, Implen, Germen), and the PrimeScript RT Reagent Kit (EZBiosciences, USA) was employed to synthesize complementary DNA (cDNA). The primers were designed using PrimerBank (Massachusetts General Hospital). qRT–PCR was performed in a 10 μL reaction mixture (cDNA sample, SYBR Green qPCR SuperMix reagent, and primers). The samples underwent two-step amplification with an initial step at 95°C (3 min), followed by 95°C (3 s) and 60 °C (31 s) for 40 cycles. mRNA expression was quantified by the $2^{-\Delta\Delta}$CT analytical method on a CFX Connect™ Real-Time PCR Detection System Flier (Bio-Rad CFX Connect, USA). The untreated 231 cells were used as negative controls. The mRNA level of the GAPDH gene was measured as an internal normalization standard. The sequences of the primers were detailed in Table1.

ISSN 2616-5791 Vol.5, Issue 5: 7-12, DOI: 10.25236/AJMHS.2024.050502

Table 1: The sequences of the primers for qRT-PCR

Gene	Forward primer, 5′- 3′	Reverse primer 5′- 3′
HIF-1α	GAACGTCGAAAAGAAAAGTCTCG	CCTTATCAAGATGCGAACTCACA
Bcl-2	GGTGGGGTCATGTGTGTGG	CGGTTCAGGTACTCAGTCATCC
GAPDH	GAACGGGAAGCTCACTGG	GCCTGCTTCACCACCTTCT

Immunofluorescence assays: Immunofluorescence assays were performed to examine the expression of Tubulin. In brief, 231 cells were seeded in confocal dishes at a density of 1 × 10^4 cells/dish for 24 h at 37°C under 5% CO2. After seeding, the cells were incubated with DMM or PBS under normaxia or hypoxia conditions for 12 h. Then, the cells were collected and fixed with 4% paraformaldehyde for 30 min a, and then the samples were incubated with Tubulin antibody (1:500, Invitrogen) for 2 hours at 37 °C. Then, the cells were incubated with the corresponding secondary antibodies (ab2762824, Invitrogen) for 2 hours at 37 °C for fluorescent labeling. Finally, the cell nuclei were stained with DAPI for 5 minutes. Immunofluorescence images were observed and captured using Confocal laser scanning microscope (CLSM).*Cell Cytotoxicity Assay:* MCF-10A, MDA-MB-231 cells and MCF-7 cells were incubated in 96-well plates at a density of 1 × 10^4 cells/well for 24 h and then treated with different concentrations of DM and DMM respectively, for another 12 h at 37 °C under 5% CO2. Then the plates were washed with PBS twice to remove the excess nanocarriers adsorbed onto cell membranes. CCK- 8 solution (100 μL) was added to each plate for 2 h of incubation. Then the UV absorption at 450 nm of each well was measured. All the experiments were performed in triplicate, and five wells were used in each group.

3. Results and discussion

RT-PCR results showed the expression of Bcl-2 mRNA in MDA-MB-231 cells with PBS treatment was significantly higher than that treated with DATS. After incubation of 100 μMMM and DMM with MDA-MB-231 cells for 24 hours, the expression of Bcl-2 mRNA in the cells decreased by 32% and 23.77%, respectively ($p<0.05$, Figure 1). These finding suggested MM and DMM can reduce the expression of Bcl-2 mRNA in breast cancer and promote tumor cell apoptosis. The expression of HIF-1a mRNA in MDA-MB-231 cells with PBS treatment was significantly higher in normoxic and hypoxic conditions, and the expression of HIF-1a mRNA in untreated MDA-MB-231 cells was about 24% higher than that in normoxic conditions. After incubation of 50 μM and 150 μM DMM with MDA-MB-231 cells for 24 hours resulted in a 14.6% and 43% decrease in intracellular HIF-1a mRNA expression, respectively ($p<0.05$ and $p<0.001$); When 150 μ M DMM was incubated with MCF-7 cells for 24h, the expression of HIF-1a mRNA in MDA-MB-231 decreased by 76.12% ($p<0.0001$). These finding indicated that DMM can reduce the expression of HIF-1a mRNA in breast cancer and improve the hypoxic microenvironment of the tumor.

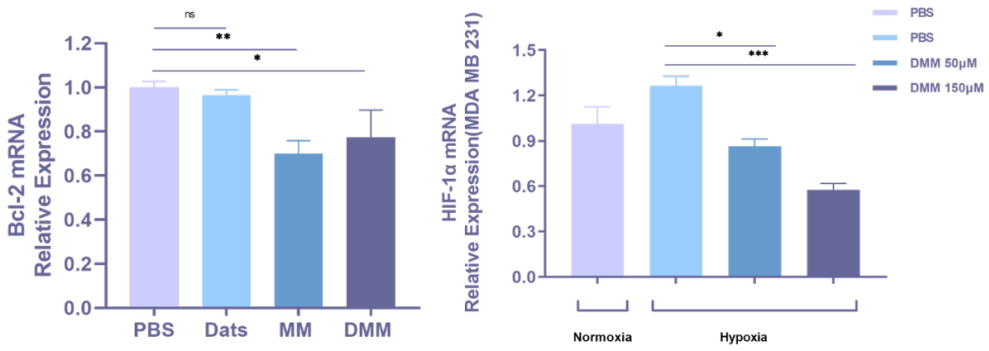

Figure 1: qRT-PCR analysis of the expression of Bcl-2 and HIF-1α mRNA in macrophages activated by inflammasomes after treatment with DATS, MM, and DMM.

As shown in Figures 2, the survival rates of MDA-MB-231, MCF7, and MCF10A cells treated with different concentrations and nanomedicines were measured using CCK8. After treatment with MM and DMM (100 μM), the survival rates of MDA-MB-231 cells were 62.12% and 32.59%, respectively, and the survival rates of MCF7 cells were 50.93% and 55.40%, respectively. After treatment with 150 μM MM and DMM, the survival rates of MDA-MB-231 cells were 50.14% and 35.01%, respectively. The viability of MCF7 cells was observed for 34.71% and 33.32% respectively. It shows that when the

ISSN 2616-5791 Vol.5, Issue 5: 7-12, DOI: 10.25236/AJMHS.2024.050502

concentration of nanomaterials MM and DMM is 100-150 μM, the survival rate of MDA-MB-231 and MCF7 tumor cells is significantly reduced, while the survival rate of MCF10A cells treated with 1-150 μ M nanomaterials can reach more than 79%, indicating that nanomaterials with a certain concentration have a significant killing effect on MDA-MB-231 and MCF7 breast cancer cells, but have no significant impact on the activity of MCF10A.

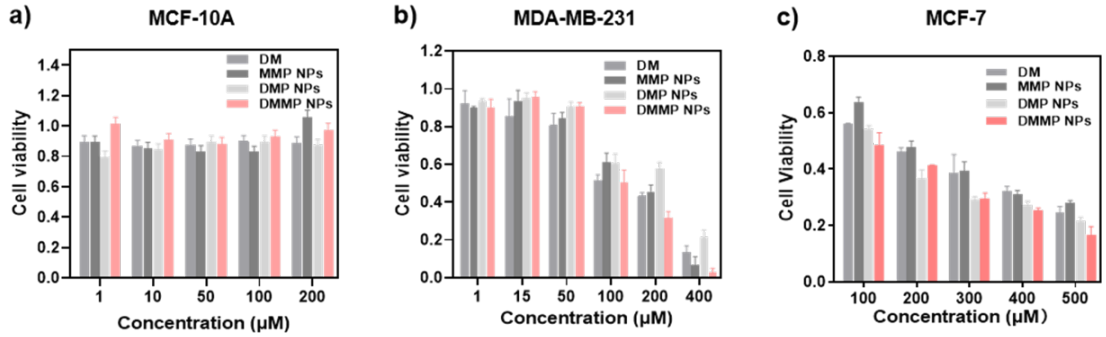

Figure 2: The viability of MDA-MB-231, MCF7, and MCF10A cells treated with different concentrations and nanomedicines were measured using CCK8.

The results of CLSM show that untreated MDA-MB-231, MCF-7, and MCF-10A cell membranes can be stained with Tubulin labeled strip-shaped microtubule proteins, with intact cytoskeleton and plump cell morphology (Figure 3). The microtubule proteins of MDA-MB-231 and MCF-7 cells treated with DMM were damaged, losing their normal linear morphology, becoming blurry and incomplete, and the cytoskeleton was disrupted. DMM did not disrupt the cytoskeleton of MCF-10A cells.

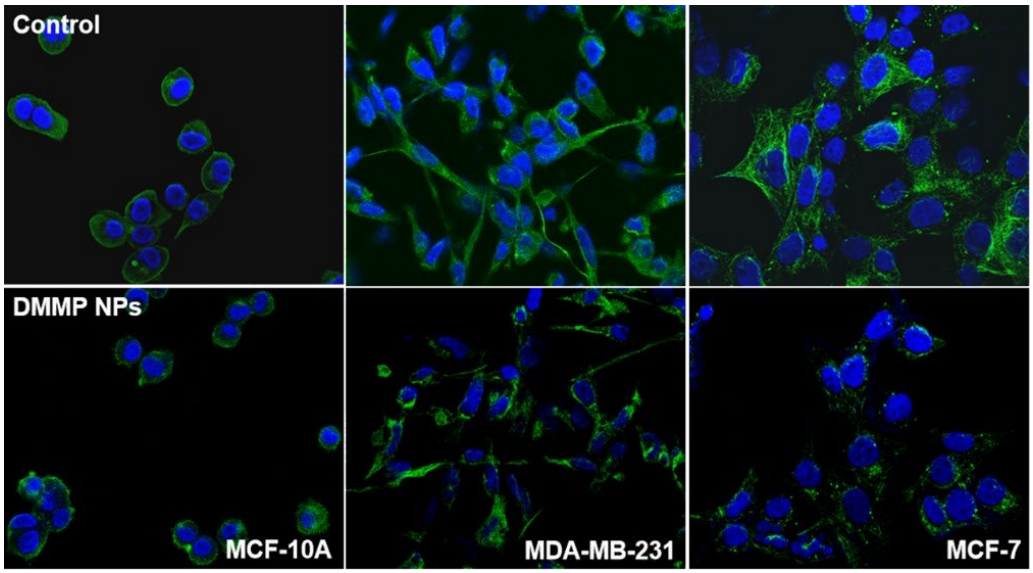

Figure 3: CLSM images showing the expression of Tubulin proteins and cell membranes morphology in MDA-MB-231, MCF-7, and MCF-10A cell after treatment with DMM. Cells were stained to label the cell nuclei with DAPI (blue).Tubulin were visualized as green.

When the PBS and MM groups were not irradiated with 450nm laser, only weak green fluorescence could be seen in the cytoplasm. After being irradiated with 450nm laser, a small amount of light green fluorescence could be seen in the cytoplasm of the PBS group, with little change compared to the negative control group; After irradiation with 450nm laser, a large amount of green fluorescence was observed in the cytoplasm of the MM group containing nanomedicines, indicating the generation of a large amount of singlet oxygen (ROS) (Figure 4).

ISSN 2616-5791 Vol.5, Issue 5: 7-12, DOI: 10.25236/AJMHS.2024.050502

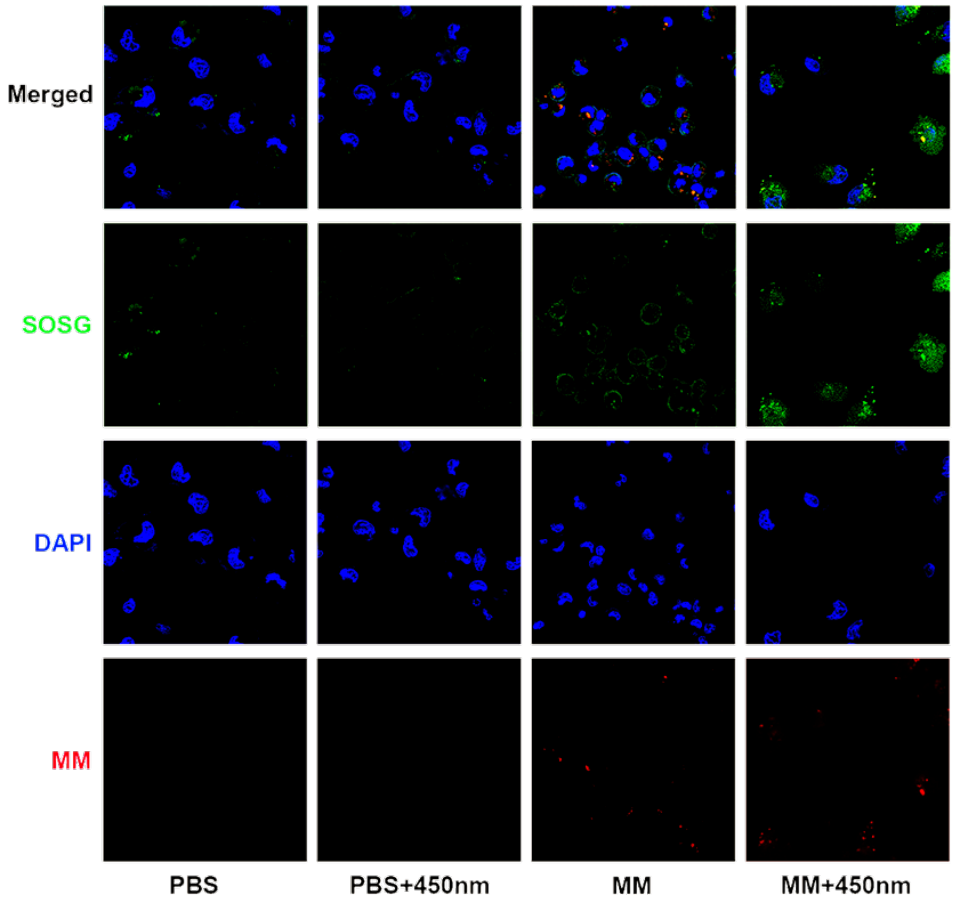

Figure 4: CLSM images showing the expression of SOSG in MDA-MB-231 after treatment with DMM and PDT. Cells were stained to label the cell nuclei with DAPI (blue). ROS were visualized as green by SOSG. DMM were visualized as red. Excitation wavelength λex, 400nm; emission wavelength λem, 610nm

4. Conclusion

The nanodrugs based on the hollow mesoporous MnO2 is loaded with MOC, and the nanodrugs loaded with DATS (DMM) that has the ability to target the tumor microenvironment and release O2. It can combine with photodynamic therapy to produce large amounts of singlet oxygen and inhibit tumor growth. The load DATS have synergistic effect. At the same time, it has good biological safety.

References

[1] Dai X, Xiang L, Li T, Bai Z. Cancer Hallmarks, Biomarkers and Breast Cancer Molecular Subtypes. J Cancer. 2016 Jun 23; 7(10):1281-94.
[2] Asleh K, Riaz N, Nielsen TO. Heterogeneity of triple negative breast cancer: Current advances in subtyping and treatment implications. J Exp Clin Cancer Res. 2022 Sep 1; 41(1):265.
[3] Huang Y, Zheng C, Zhang X, Cheng Z, Yang Z, Hao Y, Shen J. The Usefulness of Bayesian Network in Assessing the Risk of Triple-Negative Breast Cancer. Acad Radiol. 2020 Dec; 27(12):e282-e291.
[4] Bianchini G, Balko JM, Mayer IA, Sanders ME, Gianni L. Triple-negative breast cancer: challenges and opportunities of a heterogeneous disease. Nat Rev Clin Oncol. 2016 Nov; 13(11):674-690.
[5] Li Y, Zhang H, Merkher Y, Chen L, Liu N, Leonov S, Chen Y. Recent advances in therapeutic strategies for triple-negative breast cancer. J Hematol Oncol. 2022 Aug 29; 15(1):121.
[6] Geisler, S.; Lønning, P.E.; Aas, T.; Johnsen, H.; Fluge, O.; Haugen, D.F.; Lillehaug, J.R.; Akslen, L.A.; Børresen-Dale, A.L. Influence of TP53 gene alterations and c-erbB-2 expression on the response to treatment with doxorubicin in locally advanced breast cancer. Cancer Res. 2001, 61, 2505–2512.
[7] Maker, A.V.; Attia, P.; Rosenberg, S.A. Analysis of the cellular mechanism of antitumor responses

ISSN 2616-5791 Vol.5, Issue 5: 7-12, DOI: 10.25236/AJMHS.2024.050502

and autoimmunity in patients treated with CTLA-4 blockade. J. Immunol. 2005, 175, 7746–7754.
[8] de Visser KE, Joyce JA. The evolving tumor microenvironment: From cancer initiation to metastatic outgrowth. Cancer Cell. 2023 Mar 13; 41(3):374-403.
[9] Cheung EC, Vousden KH. The role of ROS in tumour development and progression. Nat Rev Cancer. 2022 May; 22(5):280-297.
[10] Jin F, Wu Z, Hu X, Zhang J, Gao Z, Han X, Qin J, Li C, Wang Y. The PI3K/Akt/GSK-3β/ROS/eIF2B pathway promotes breast cancer growth and metastasis via suppression of NK cell cytotoxicity and tumor cell susceptibility. Cancer Biol Med. 2019 Feb; 16(1):38-54.
[11] Ren Y, Lin Y, Chen J, Jin Y. Disulfiram Chelated with Copper Promotes Apoptosis in Osteosarcoma via ROS/Mitochondria Pathway. Biol Pharm Bull. 2021; 44(10):1557-1564.
[12] Dekker Y, Le Dévédec SE, Danen EHJ, Liu Q. Crosstalk between Hypoxia and Extracellular Matrix in the Tumor Microenvironment in Breast Cancer. Genes (Basel). 2022 Sep 3; 13(9):1585.
[13] Cheng SY, Yang YC, Ting KL, Wen SY, Viswanadha VP, Huang CY, Kuo WW. Lactate dehydrogenase downregulation mediates the inhibitory effect of diallyl trisulfide on proliferation, metastasis, and invasion in triple-negative breast cancer. Environ Toxicol. 2017 Apr; 32(4):1390-1398.
[14] de Heer EC, Jalving M, Harris AL. HIFs, angiogenesis, and metabolism: elusive enemies in breast cancer. J Clin Invest. 2020 Oct 1; 130(10):5074-5087.
[15] Yang B, Chen Y, Shi J. Tumor-Specific Chemotherapy by Nanomedicine-Enabled Differential Stress Sensitization. Angew Chem Int Ed Engl. 2020 Jun 8; 59(24):9693-9701.
[16] Ostańska E, Aebisher D, Bartusik-Aebisher D. The potential of photodynamic therapy in current breast cancer treatment methodologies. Biomed Pharmacother. 2021 May; 137:111302.
[17] Agostinis P, Berg K, Cengel KA, Foster TH, Girotti AW, Gollnick SO, Hahn SM, Hamblin MR, Juzeniene A, Kessel D, Korbelik M, Moan J, Mroz P, Nowis D, Piette J, Wilson BC, Golab J. Photodynamic therapy of cancer: an update. CA Cancer J Clin. 2011 Jul-Aug;61(4):250-81.
[18] Korbelik M. PDT-associated host response and its role in the therapy outcome. Lasers Surg Med. 2006 Jun; 38(5):500-8.
[19] Malla R, Marni R, Chakraborty A, Kamal MA. Diallyl disulfide and diallyl trisulfide in garlic as novel therapeutic agents to overcome drug resistance in breast cancer. J Pharm Anal. 2022 Apr;12(2):221-231.
[20] Chen H, Guan X, Liu Q, Yang L, Guo J, Gao F, Qi Y, Wu X, Zhang F, Tian X. Co-assembled Nanocarriers of De Novo Thiol-Activated Hydrogen Sulfide Donors with an RGDFF Pentapeptide for Targeted Therapy of Non-Small-Cell Lung Cancer. ACS Appl Mater Interfaces. 2022 Dec 7; 14(48): 53475-53490.